Opsonisation of nanoparticles prepared from poly(β-hydroxy butyrate)- and poly(trimethylene carbonate)-*b*-poly(malic acid) amphiphilic diblock copolymers: Impact on the *in vitro* cell uptake by primary human macrophages and HepaRG hepatoma cells

Vene Elise[1†], Barouti Ghislaine[2†], Jarnouen Kathleen[1], Gicquel Thomas[1], Claudine Rauch[1], Ribault Catherine[1], Guillaume Sophie M.[2], Cammas-Marion Sandrine[3], Loyer Pascal[1]*

[1]INSERM UMR S-991, Foie, Métabolismes et Cancer ; Université de Rennes 1 ; CHU Pontchaillou Rennes, 35033 Rennes, France.

[2]Institut des Sciences Chimiques de Rennes ; UMR 6226 CNRS ; Université de Rennes 1, Campus de Beaulieu, 263 Avenue du Général Leclerc, F-35042 Rennes Cedex, France

[3]Ecole Nationale Supérieure de Chimie de Rennes ; Institute des Sciences Chimiques de Rennes; Université de Rennes 1, 11 allée de Beaulieu, CS 50837, 35708 Rennes Cedex 7, France.

Corresponding author: Pascal Loyer (pascal.loyer@univ-rennes1.fr)

[†]These authors contributed equally to this work

Graphical abstract

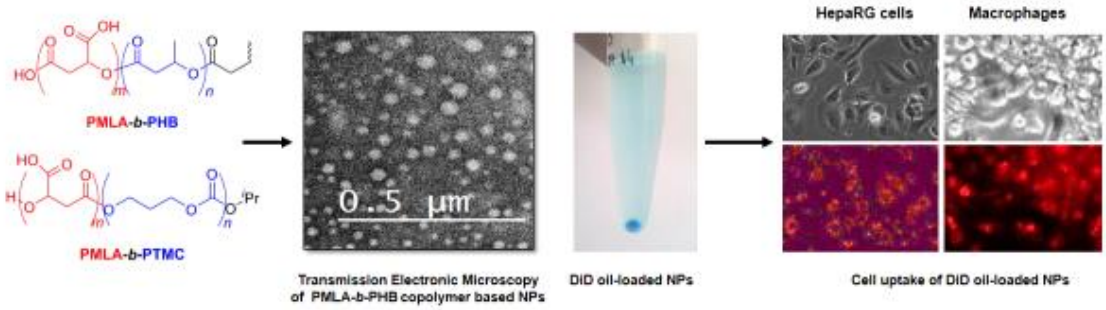

ABSTRACT

The present work reports the investigation of the biocompatibility, opsonisation and cell uptake by human primary macrophages and HepaRG cells of nanoparticles (NPs) formulated from poly(β-malic acid)-*b*-poly(β-hydroxybutyrate) (PMLA-*b*-PHB) and poly(β-malic acid)-*b*-poly(trimethylene carbonate) (PMLA-*b*-PTMC) diblock copolymers, namely $PMLA_{800}$-*b*-PHB_{7300}, $PMLA_{4500}$-*b*-PHB_{4400}, $PMLA_{2500}$-*b*-$PTMC_{2800}$ and $PMLA_{4300}$-*b*-$PTMC_{1400}$. NPs derived from PMLA-*b*-PHB and PMLA-*b*-PTMC do not trigger lactate dehydrogenase release and do not activate the secretion of pro-inflammatory cytokines demonstrating the excellent biocompatibility of these copolymer derived nano-objects. Using a protein adsorption assay, we demonstrate that the binding of plasma proteins is very low for PMLA-*b*-PHB-based nano-objects, and higher for those prepared from PMLA-*b*-PTMC copolymers. Moreover, a more efficient uptake by macrophages and HepaRG cells is observed for NPs formulated from PMLA-*b*-PHB copolymers compared to that of PMLA-*b*-PTMC-based NPs. Interestingly, the uptake in HepaRG cells of NPs formulated from $PMLA_{800}$-*b*-PHB_{7300} is much higher than that of NPs based on $PMLA_{4500}$-*b*-PHB_{4400}. In addition, the cell internalization of $PMLA_{800}$-*b*-PHB_{7300} based-NPs, probably through endocytosis, is strongly increased by serum pre-coating in HepaRG cells but not in macrophages. Together, these data strongly suggest that the binding of a specific subset of plasmatic proteins onto the $PMLA_{800}$-*b*-PHB_{7300}-based NPs favors the HepaRG cell uptake while reducing that of macrophages.

Keywords: poly(trimethylene carbonate), poly(hydroxy alkanoate), poly(malic acid), nanoparticle, macrophages, HepaRG cells.

INTRODUCTION

The development of new drugs, at least in the past few decades, has been focused on the identification of compounds inhibiting/activating molecular target(s); however, the pharmaceutical research most commonly has not yet taken into account site-specific delivery. As a consequence, most actual chemotherapeutics do not accumulate specifically at sites of interest. In contrast, drugs distribute evenly throughout the body, often resulting in deleterious side-effects in healthy organs, in their rapid metabolism and elimination by the liver and kidney, and in a limited bioavailability. The inability to address chemotherapies to target tissues and/or to maintain sufficient plasma drug concentration, significantly contributes to the retrieval of promising molecules and the lack of efficacy of approved drugs (Kola and Landis, 2004; Blanco et al., 2015).

To overcome these limitations, the design of nanoparticles (NPs) embedding the drugs has appeared as a suitable strategy in order to prevent the rapid elimination of therapeutic payloads and to achieve a prolonged plasma drug concentration (Torchilin, 2006; Cabral et al., 2014). Academic laboratories and pharmaceutical companies have produced many synthetic NPs, but only few formulations have obtained approval by regulatory authorities and reached the market and clinical practice because of their limited efficacy and/or concerns about their clinical safety (Editorial, 2014; Raemdonck and De Smedt, 2015). However, notable examples are used in clinical protocols such as Doxil® (O'Brien et al., 2004), a liposome encapsulating doxorubicin, and Abraxane® (Stinchcombe, 2007), an albumin NP loaded with paclitaxel, which confirm the obvious potential for increased bioavailability and tumor targeting. Despite these successes, the use of drug delivery nanostructures in clinical protocols is far from being a generalized routine and optimizations of NPs are required to overcome biological barriers and to address cellular targets (Blanco et al., 2015).

Following systemic administration, NPs are subjected to the opsonization, the non-specific interactions with plasma proteins, and the recognition by antibodies and proteins of the complement system (Frank and Fries, 1991; Owens and Peppas, 2006; Tenzer et al., 2013), which is part of the innate immune system enhancing the activity of the mononuclear phagocyte system (MPS) to clear pathogens from the body. In order to minimize the opsonisation and the non-specific scavenging by MPS, NPs' features have been optimized through the modulation of their size, shape (Blanco et al., 2015), surface charge (Arvizo et al., 2011) and chemical structure (Moghini et al., 2001; Nel et al., 2009; Mahon et al., 2012). Moreover, NP platforms

developed for the profit of drug-delivery systems often include a poly(ethylene glycol) (PEG) chain of various length resulting in the "stealth" behavior of the corresponding PEG-based NPs towards opsonins and extending their systemic lifetime (Owens and Peppas, 2006; Tenzer et al., 2013). Indeed, the PEG segments associated to water molecules form a hydrating layer (Harris and Chess, 2003), which acts as a steric shield to prevent the binding of serum opsonins and delay the uptake by MPS. Furthermore, the PEG corona often increases the hydrodynamic diameter of the NPs thereby decreasing the renal clearance (Veronese, 2001). PEG, however, is not immunologically inert since it was reported that serum of healthy blood donors often contain anti-PEG immunoglobulins most likely due to exposure to PEG during their life (Richter, A.W. and Akerblom, 1984; Ishida et al., 2006). In addition, the unpredicted clearance times of PEGylated compounds lead to accumulation of high molecular weight compounds in the liver (Dams et al., 2000) with unknown toxicological consequences over a long period of time (Kawai, 2002). Some studies have evaluated other water-soluble polymers in order to overcome the limitations in the use of PEG (Kierstead et al., 2015). For instance, poly[*N*-(2-hydroxypropyl) methacrylamide] (Lammers and Ulbrich, 2010) and poly(vinylpyrrolidone) (Zelikin et al., 2007; Kierstead et al., 2015) coatings on liposomes also demonstrated the ability to extend circulation times and to avoid accelerated blood clearance although their opsonisation by plasma proteins remains poorly documented.

The second major biological barrier for the NPs to overcome is the continuous endothelium of the blood vessels. The discovery of the Enhanced Permeability and Retention effect (EPR) (Matsumura and Maeda, 1986) defining the extravasation of macromolecules and nanovectors through the fenestrated blood vessels within solid tumors, has opened the perspective for improved therapeutic indexes of vectorized chemotherapies (Maeda et al., 2013 ; Maeda et al., 2016). Indeed, the presence of disorganized and/or fenestrated vasculature endothelium favors the accumulation of NPs in solid tumors and, to a lesser extent, at sites of injury, infection or inflammation, and heightens the drug concentration in these specific microenvironments (Azzopardi et al., 2013; Blanco et al., 2015). The rationale for drug delivery using NPs thus mainly arises from this EPR-mediated passive targeting, (Blanco et al., 2015) and more recently from strategies of active targeting relying on the design of NP surfaces tagged with moieties specifically binding to membrane receptors overexpressed on tumor cells and/or the surrounding angiogenic vessels (Dawidczyk et al., 2014). However, after injection and opsonization, most NPs accumulate in the liver and spleen because of their specific vasculature, and of the capillary network with endothelial fenestrations and venous sinuses, respectively.

The liver sinusoids are highly specialized capillaries harboring large fenestrations in the endothelium and lacking basal lamina, which enhances the exchange between the liver parenchyma and the blood stream coming from the digestive tract and the hepatic artery (Jacobs et al., 2010). The hepatic architecture greatly favors the accumulation of NPs within the space of Disse where they are in close contact with the hepatocytes and the liver resident macrophages, namely the Kupffer cells (Blanco et al., 2015). This very active compartment of the MPS within the liver parenchyma reduces the targeting of the hepatocytes and impairs the use of nanotechnology-based therapy of hepatocyte diseases including hepatocellular carcinoma (HCC). In addition, the uptake of NPs by Kupffer cells may activate the inflammasome, a major factor of the innate immune system involved in the production of pro-inflammatory cytokines (Baron et al., 2015). Conversely, authors have taken advantage of the highly active phagocytic activity of Kupffer cells to specifically deliver anti-infectious therapeutics to hepatic macrophages infected with microorganisms such as leishmaniasis (Alving et al., 1978) and salmonellosis (Fattal et al., 1989). In this context, the development of NPs which would favor the cell uptake of either the hepatocytes or the Kupffer cells is of particular interest for the treatment of liver diseases (Reddy and Couvreur, 2011; Zhang et al. 2016).

Amphiphilic block copolymers self-assemble in aqueous solution to form NPs with a hydrophilic corona and a hydrophobic inner-core particularly well-adapted for drug encapsulation and delivery. The synthesis of copolymers providing biocompatible and highly stable self-assembled systems is particularly challenging. Indeed, the choice of the hydrophobic block strongly impacts the physico-chemical properties of the resulting self-assembled systems such as the hydrodynamic radius and the critical micelle concentration (CMC) which are two key parameters. Poly(hydroxyalkanoates) (PHAs) and poly(carbonates) (PCs) have attracted considerable attention for the design of drug delivery systems due to their high biocompatibility and low toxicity (Furrer et al., 2008; Wu et al., 2009; Hazer, 2010; Hu et al., 2012; Shrivastav et al., 2013; Chen et al., 2014; Loyer and Cammas-Marion, 2014; Li and Loh, 2015; Nigmatullin et al., 2015). In this context, poly(3-hydroxybutyrate) and poly(trimethylene carbonate) have been developed to produce gels and matrices for tissue engineering (Shishatskaya et al., 2004 ; Asran et al., 2010 ; Song et al., 2011 ; Schüller-Ravoo et al., 2013 ; Rozila et al., 2016 ; Ding et al., 2016 ; Pascu et al., 2016 ; Zant et al., 2016) and NPs for drug delivery (Xiong et al., 2010 ; Jiang et al., 2013 ; Fukushima 2016 ; Pramual et al., 2016). Our laboratories have recently synthesized and characterized novel poly(hydroxyalkanoate)-based

amphiphilic diblock copolymers, namely poly(β-malic acid)-*b*-poly(3-hydroxybutyrate) (PMLA-*b*-PHB) (Barouti et al., 2015) and poly(β-malic acid)-*b*-poly(trimethylene carbonate) (PMLA-*b*-PTMC) (Barouti et al., 2016a), hydrophobic $PMLA^{Be}$-*b*-PHB-*b*-$PMLA^{Be}$ and amphiphilic PMLA-*b*-PHB-*b*-PMLA triblock copolymers (Barouti et al., 2016b) as well as linear and star-shaped thermogelling poly([R]-3-hydroxybutyrate) copolymers (Barouti et al., 2016c). One of the objectives was to elaborate biocompatible and biodegradable copolymer-based NPs, and more importantly to highlight the impact of the chemical structure of the hydrophobic block and the influence of the hydrophilic weight fraction on the physico-chemical properties of the self-assembled systems. In these studies, PMLA was used as the hydrophilic block due to its complete biodegradability, and its better biocompatibility as compared to PEG, while PHB and PTMC with a chemically distinct functionality (ester vs carbonate, respectively) were used as the hydrophobic block (Figure 1). The synthesis of these copolymers was performed by the controlled ring-opening polymerization of the monomers affording well-defined PMLA-*b*-PHB and PMLA-*b*-PTMC copolymers ranging from PMLA-enriched to longer hydrophobic (PHB, PTMC) segment and featuring finely tuned macromolecular features (Table 1). Our previous results on the evaluation of the biocompatibility of the NPs prepared from these diblock copolymers using human HepaRG hepatocyte-like cells and the 3-(4,5-dimethylthiazol-2-yl)-2,5-diphenyltetrazolium bromide (MTT) assays, revealed no significant effect on cells viability at low concentrations, and very mild cytotoxicity at high concentrations (Barouti et al., 2015; Barouti et al., 2016).

In the present work, we have further investigated the biocompatibility of NPs formulated from two PMLA-*b*-PHB and two PMLA-*b*-PTMC diblock copolymers featuring different hydrophilic fraction (*f*), namely $PMLA_{800}$-*b*-PHB_{7300} (*f* = 10%), $PMLA_{4500}$-*b*-PHB_{4400} (*f* = 51%), $PMLA_{2500}$-*b*-$PTMC_{2800}$ (*f* = 47%) and $PMLA_{4300}$-*b*-$PTMC_{1400}$ (*f* = 75%) (Table 1), by investigating the cell uptake and the inflammasome activation level in human primary macrophages and HepaRG cells of these NPs. The opsonisation of NPs derived from these copolymers was also evaluated. The aim of this study was first to investigate the influence of the chemical structure (ester or carbonate) of the hydrophobic block of the copolymer and then the influence of the hydrophilic weight fraction on the biological parameters, in order to identify the optimal NPs that would provide the most interesting self-assembled systems by favoring the uptake by hepatocytes and reducing that of macrophages.

MATERIALS AND METHODS

Materials

The hydrodynamic diameter and the polydispersity of the micelles were measured by Dynamic Light Scattering (DLS) according to the CONTIN method, using a Delsa™ Nano Beckman Coulter apparatus at 25 °C.

The zeta potential measurements were performed on a Delsa™ Nano Beckman Coulter apparatus at 25 °C. Laser Doppler electrophoresis in phase mode was conducted with sequential fast and slow field reversal, applying a potential of ±150 V. The measured electrophoretic mobility (μ) was then converted to zeta potential (ζ) using the Smoluchowski approximation.

The UV spectra were recorded on a Secoman apparatus at 670 nm.

The cell uptake of fluorescent NPs labelled with the lipophilic fluorescent dye 1,1′-dioctadecyl-3,3,3′,3′-tetramethylindodicarbocyanine perchlorate (DiD oil; Thermofisher Scientitic, Wavelength: excitation 644 nm; emission 665 nm, ε = 236.000) was quantified by flow cytometry using FACSCalibur (Becton Dikinson). Cytometry data were analyzed using CellQuest Software (Becton Dikinson).

For cytotoxicity assays, the optical absorbance was measured on a microplate reader Multiskan FC (ThermoScientific) at 492 for both the LDH and MTT assays.

Electrophoresis and protein transfers were performed on XCell SureLock™ and iBlot2® apparatus (Life Technologies). Acquisitions of gels stained with coomassie blue and immunoblotting detection by chemioluminescence were performed using VisionCapt and Chemi-Smart 5000 systems (Vilber Lourmat), respectively.

Reagents

Phosphate-buffered saline (PBS), William's E medium, RPMI 1640, penicillin–streptomycin, L-glutamine and trypsin were purchased from ThermoFisher Scientific (Saint Aubin, France). Fetal calf serum (FCS) FetalClone III® and BioWhittaker® were from Hyclone (Logan, UR, USA) and Lonza (Verviers, Belgium), respectively. Hydrocortisone hemisuccinate was from Serb (Paris, France). MOPS-SDS buffer was purchased from Amresco (OH, USA). Tris-buffered saline (TBS) was from GE Healthcare (Aulnay Sous Bois, France). Bovine serum albumin was from Eurobio (Les Ulis, France). Ultrapure Escherichia coli O111:B4 LPS was purchased from InvivoGen (Toulouse, France) and recombinant human granulocyte macrophage colony-stimulating factor (rhGM-CSF) from R&D Systems Europe

(Lille, France). Lactate dehydrogenase (LDH) and insulin were obtained from Sigma-Aldrich (Saint Louis, MO, USA). Carboxylate-modified fluorescent (yellow-green) microspheres FluoSpheres® (20 and 100 nm) and 1,1′-dioctadecyl-3,3,3′,3′-tetramethylindodicarbocyanine perchlorate (DiD oil) were purchased from Molecular Probes (Eugene, OR, USA). Monosodium urate (MSU) crystals were prepared by recrystallization from uric acid, as previously described (Gicquel et al., 2015). Genistein and Chlorpromazin were purchased from Sigma-Aldrich. Antibodies, goat antiserum to human albumin (1140V7) and goat anti-human transferrin (1205Y2) were from Kent Laboratories (Redmond, WA, USA), rabbit immunoglobulins to human fibrinogen (A080) and horse radish peroxidase labeled secondary antibodies were from Dako (Denmark), rabbit anti-complement C3 (sc-31300) was from Santa Cruz (distributed by CliniSciences, Nanterre, France) and anti-human immunoglobulins was purchased from Amersham (RPN 1003).

Preparation of PMLA-b-PHB and PMLA-b-PTMC based micelles

The $PMLA_{800}$-*b*-PHB_{7300}, $PMLA_{4500}$-*b*-PHB_{4400}, $PMLA_{2500}$-*b*-$PTMC_{2800}$ and $PMLA_{4300}$-*b*-$PTMC_{1400}$ copolymers were synthesized by the sequential ring-opening polymerization (ROP) of β-butyrolactone, benzyl β-malolactonate, and trimethylene carbonate. The subsequent hydrogenolysis of these hydrophobic copolymers afforded the corresponding amphipihilic PMLA-*b*-PHB and PMLA-*b*-PTMC copolymers (Barouti et al., 2015; Barouti et al., 2016). The resultant empty macromolecular micelles were prepared by the nanoprecipitation method (Thioune et al., 1997) as previously established (Barouti et al., 2015; Barouti et al., 2016). The NPs were then analyzed by DLS for hydrodynamic diameter, polydispersity and zeta potential measurements (Table 1).

The 1,1′-dioctadecyl-3,3,3′,3′-tetramethylindodicarbocyanine perchlorate (DiD oil) loaded NPs were prepared using the nanoprecipitation procedure using 1% (*wt*/*wt*) of the DiD oil fluorescent probe dissolved in acetone (2 mg/mL) added to the acetone solution of the block copolymer (5 mg) to an ultimate volume of 1 mL. Following the organic solvent evaporation, the unloaded DiD oil was removed by filtration through a sephadex PD 10 column. The volume of the recovered solution was completed to 2.5 mL with distilled water in order to obtain a final concentration in NPs of 2 mg/mL. The concentration of loaded DiD oil was evaluated by UV at 660 nm using a calibration curve of DiD oil solution in a mixture of DMF/H_2O (80/20, *v*/*v*). The DiD oil-loaded NPs (80 µL) were mixed with DMF (320 µL) and the resulting solution was analyzed by UV to measure the encapsulation efficiency (EE) calculated using the following equation: $EE\ (\%) = [\text{DiD oil}]_{encapsulated}/[\text{DiD oil}]_0 \times 100$.

Opsonisation of PMLA-b-PHB and PMLA-b-PTMC based NPs

The opsonisation of NPs formulated from $PMLA_{800}$-*b*-PHB_{7300}, $PMLA_{4500}$-*b*-PHB_{4400}, $PMLA_{2500}$-*b*-$PTMC_{2800}$ and $PMLA_{4300}$-*b*-$PTMC_{1400}$ diblock copolymers was studied using a protein adsorption assay. NPs were incubated with human serum prior to the detection of micelle-bound proteins using electrophoresis on acrylamide gels. Briefly, various amounts of copolymers resulting in the same specific NP surface were diluted in PBS (0.5 mL) then mixed with human serum (0.5 mL) for time periods ranging from 5 min to 16 h at 37 °C. NPs were then collected by centrifugation at 14,000 g for 30 min. The pellet was washed twice with cold PBS (1 mL) prior to denaturation of micelles and bound proteins with loading buffer (100 µL; Tris-HCl 100 mM, pH 6.8, bromophenol blue 0.2%, sodium dodecyl sulfate 8%, glycerol 20 %, and β-mercaptoethanol 5%). Samples were boiled in water bath for 10 min, then proteins were loaded on 10% polyacrylamide gels (Novex®, Life Technologies) and separated by electrophoresis. Standard PageRuler™ Plus Prestained Protein Ladder (Fermentas) was run in parallel. Total proteins were detected by coomassie blue dye staining or immunoblotting following transfer onto nitrocellulose membranes (iBlot® gel transfer stack nitrocellulose, Novex® Life Technologies) using anti-albumin, -transferrin, -fibrinogen, -immunoglobulin and -complement C3 specific antibodies.

For immunoblotting, nonspecific binding sites were blocked with Tris-buffered saline (TBS) containing 4% bovine serum albumin for 1 h at room temperature. Then membranes were incubated overnight at 4°C with primary antibodies diluted at 1:2000 in TBS containing 4% advanced blocking agent (GE Healthy Care). Membranes were washed 3 times with TBS and incubated with appropriate secondary antibody conjugated to horseradish peroxidase diluted at 1:5000 in TBS containing 0.2% Tween 20 and 4% advanced blocking agent for 1 h at room temperature. The proteins were visualized with Supersignal (Pierce, Rockford, IL, USA).

Cell culture and cell uptake of NPs

HepaRG cells were plated at a density of 0.1 x 10^6 cells per well in 24-well plates and cultured as previously described (Corlu and Loyer, 2015) in William's E medium supplemented with 2 mM of glutamine, 100 IU/ml penicillin–100 mg/ml streptomycin, 5 mg/L of insulin, 10^{-5} M hydrocortisone hemisuccinate and 10% of fetal calf serum (FCS) FetalClone III®, at 37 °C with 5% humidified CO_2.

Peripheral blood mononuclear cells were obtained from two human buffy coat (Etablissement Français du Sang, Rennes, France) by differential centrifugation on UNI-SEP maxi U10 (Novamed, Jerusalem, Israel). The experiments were performed in compliance with the French legislation on blood donation and blood products' use and safety. Monocytes from healthy donors were enriched using a human CD14 separation kit (Microbeads; Miltenyi Biotec, Bergisch Gladbach, Germany), plated at a density of 0.5 x 10^6 cells per well in 24-well plates and cultured at 37 °C with 5% humidified CO_2 in RPMI 1640 medium supplemented with 100 IU/ml penicillin–100 mg/ml streptomycin, 2 mM L-glutamine and 10% FCS BioWhittaker®. Macrophages were obtained after differentiation from monocytes by incubation with 50 ng/mL rhGM-CSF in RPMI 1640 medium during 7 days, as previously described (Gicquel et al., 2015).

For the cell uptake assay of NPs and microspheres, the culture media of human macrophages and HepaRG cells containing 10% FCS were renewed and copolymers NPs (2 μM) loaded with DiDoil or fluorescent microspheres FluoSpheres® were added to the wells overnight. For the experiments of cell uptake inhibition, cells were incubated with DiDoil-loaded $PMLA_{800}$-*b*-PHB_{7300}-based NPs for 4 h in two distinct conditions: 1) at 4 and 37°C, 2) in absence or presence of genistein (200 μM) and chlorpromazin (20 μM), as previously described (Lühmann et al., 2008). After incubation, culture media were discarded and the cell monolayers were washed once with PBS before observation by fluorescence microscopy (Zeiss Inverted Microscope, Analysis Software AxioVision). Then, cells were detached with trypsin and analyzed by flow cytometry (FACSCalibur, Becton Dikinson). Dot plots of forward scatter (FSC: x axis), the side scatter (SSC: y axis) allowed to gate the viable cells prior detecting the fluorescence emitted by the DiDoil-loaded NPs (Channel FL4-H) or fluorescent microspheres FluoSpheres® (Channel FL1-H) present in cells. Cytometry data were analyzed using the CellQuest software (Becton Dikinson).

To evaluate the influence of the opsonization on cellular uptake, the assay described above was modified by incubating DiDoil-loaded NPs or fluorescent microspheres FluoSpheres® in culture media without fetal calf serum or with the same NPs pre-incubated in human serum for 30 min at room temperature before addition to the cell media overnight at a 0.5% final concentration in human serum. The fluorescence emitted by the cells was analyzed as described above.

Cytotoxicity assay and quantification of cytokines

The lactate dehydrogenase (LDH) release was measured in the culture media following incubation with NPs using the Cytotoxicity Detection kit (Roche Diagnostics, Mannheim, Germany), according to the manufacturer's instructions. Optical absorbance was measured at 492 nm on a microplate reader (Multiskan FC, Thermo Scientific).

The cytotoxicity was also assessed using the Thiazolyl Blue Tetrazolium Bromide (MTT) assay. Briefly, cells were incubated with MTT (0.5mg/mL) for 1 h at 37 °C. The formed crystals were dissolved in DMSO at room temperature for 10 min and the absorbance was read at 490 nm with a microplate reader. The MTT values reflecting the number of viable cells were expressed in percentage relatively to the absorbance determined in control cultures.

Macrophages and HepaRG cells were incubated during 24 h with 0.1 µg/mL ultrapure lipopolysaccharide (LPS) for inflammation priming. Then, the culture media were discarded and cells were treated overnight with NPs, microspheres or MSU 250 µg/mL. Production of cytokines was evaluated by quantification of interleukin-1β (IL-1β), IL-1α and IL-6 levels in culture supernatants using Duoset ELISA kits (R&D Systems, Abingdon, United Kingdom), according to the manufacturer's instructions.

Statistical analyses

Statistical analyses were performed using a one-way Anova followed by the Kruskal–Wallis post-test or Dunn's multiple comparison tests. Statistically significant variations after treatment were compared with controls using Student's t test with Excel software. * $p < 0.05$; ** $p < 0.01$.

RESULTS

Characteristics of PHB-b-PMLA and PTMC-b-PMLA based NPs

Besides the $PMLA_{800}$-*b*-PHB_{7300}, $PMLA_{4500}$-*b*-PHB_{4400}, $PMLA_{2500}$-*b*-$PTMC_{2800}$ and $PMLA_{4300}$-*b*-$PTMC_{1400}$ amphiphilic copolymers (Figure 1), PHB_{2000} and $PTMC_{3000}$ homopolymers were also used to prepare NPs for comparative analysis of their characteristics (Table 1). The PHB and PTMC homopolymers self-assembled in PBS to form large objects (hydrodynamic diameters (D_h of 544 and 956 nm, respectively). In contrast, well-defined smaller NPs (30–130 nm) derived from PMLA-*b*-PHB and PMLA-*b*-PTMC copolymers were

formed with narrow polydispersity (PDI) (0.1 < PDI < 0.2) and a negative surface charge (−18 to −52 mV).

The lipophilic DiD oil fluorescent probe encapsulation during the self-assembly of the copolymers enabled to investigate the cell uptake of these NPs. The remaining free DiD oil was eliminated by gel filtration and the encapsulation efficiency (EE) was then measured (Table 1). PHB and PTMC homopolymers-based nano-objects encapsulated the fluorescent probe with the lowest efficiencies (EE = 19 and 14.8%, respectively) due to their inability to form well-organized self-assembled systems. For the NPs obtained from the PMLA-*b*-PHB and PMLA-*b*-PTMC copolymers, the EE increased slightly with the molar mass of the copolymers and with greater hydrophilic weight fractions (*f*; from 27.2% to 45.2% for the PMLA-*b*-PHB, and from 32.6% to 39% for the PMLA-*b*-PTMC).

In vitro cell uptake of PHB-b-PMLA and PTMC-b-PMLA based NPs

The incubation of the nano-objects was performed overnight and the macrophages and HepaRG cells uptake of PMLA-*b*-PHB and PMLA-*b*-PTMC-based NPs was monitored by the detection of the DiD oil encapsulated into the nano-objects using flow cytometry and fluorescence microscopy (Figure 2). Despite differences in the EEs of the DiD oil in the NPs derived from the different copolymers, the intensities of fluorescence were high enough to clearly distinguish negative and positive cells by microscopy and flow cytometry, as illustrated for the PMLA-*b*-PHB-based NPs (Figure 2, Supplementary data 1). Thus, the percentage of DiD oil positive cells and the intensity of fluorescence within the positive cell populations were quantified by flow cytometry (Figure 3).

With the exception of the nano-objects obtained from the PTMC homopolymer (14% and 3.25% of positive macrophages and HepaRG cells, respectively), a very efficient uptake of PHB- and copolymers-based NPs by macrophages and HepaRG cells was observed (Figure 3). Nearly 93% of macrophages were positive following incubation with objects from PHB- and $PMLA_{800}$-*b*-PHB_{7300}, and all cells were fluorescent with NPs derived from $PMLA_{4500}$-*b*-PHB_{4400}, $PMLA_{2500}$-*b*-$PTMC_{2800}$ and $PMLA_{4300}$-*b*-$PTMC_{1400}$. Similarly, the uptake by HepaRG cells was also very efficient with 94% and 85.5% of cells positive for NPs derived from PHB homopolymer and $PMLA_{800}$-*b*-PHB_{7300} copolymer, respectively, and all cells were positive with nanovectors based on $PMLA_{4500}$-*b*-PHB_{4400}, $PMLA_{2500}$-*b*-$PTMC_{2800}$ and $PMLA_{4300}$-*b*-

$PTMC_{1400}$. In contrast, less than 5% HepaRG cells were fluorescent following incubation with PTMC homopolymer-based NPs.

In contrast, the means of fluorescence reflecting the amounts of NPs within the cells were very dissimilar between the different objects and for the two cell types (Figure 3). As expected, the lowest intensities of fluorescence were observed for the PTMC homopolymer-based NPs, which triggered a limited cell uptake in macrophages and HepaRG cells. The mean of fluorescence was higher for nano-objects derived from the PHB homopolymer, which however afforded a low efficient encapsulation of the DiD oil. For the copolymer-based NPs, the intensities of fluorescence in macrophages and HepaRG cells were not correlated with the EEs of the DiD oil. The means of fluorescence in macrophages were higher with objects based on PMLA-*b*-PHB compared to those found from NPs based on PMLA-*b*-PTMC. For HepaRG cells, the highest cell uptakes were found for NPs based on PHB and $PMLA_{800}$-*b*-PHB_{7300} while $PMLA_{2500}$-*b*-$PTMC_{2800}$ and PMLA-*b*-PTMC objects led to similar cell accumulations of NPs.

The comparison of the mean values between the two cell types indicated that nano-objects of PMLA-*b*-PTMC and $PMLA_{4500}$-*b*-PHB_{4400} copolymers slightly more efficiently accumulated in macrophages than in HepaRG cells, while PHB- and $PMLA_{800}$-*b*-PHB_{7300}-based NPs favored the HepaRG cell uptake.

The significant difference in the HepaRG cell uptake between the two PMLA-*b*-PHB copolymer objects could not be explained neither by the EE of the DiD oil or by the surface charges which were nearly identical (Table 1). However, these NPs exhibit very different sizes of 130 and 30 nm, respectively, as determined by DLS, in relation to their hydrophilic weight fraction (Table 1). The size of NPs has been reported to affect the *in vitro* cell uptake in some cell types including the HepG2 hepatoma cells (Zauner et al., 2001). To determine if the cell uptake in primary human macrophages and HepaRG cells was affected by the NP size, we used green carboxylate-modified FluoSpheres® polystyrene microspheres of 100 and 20 nm and measured the cell uptake in both cell models (Figure 2). All macrophages and HepaRG cells were positive following incubation with these microspheres. In addition, the means of fluorescence were not significantly different in macrophages incubated with these microspheres of 100 and 20 nm, while a six-fold higher fluorescence was observed in HepaRG cells incubated with 100 nm microspheres as compared to the mean found for the 20 nm microspheres. Interestingly, the means of fluorescence were much higher in macrophages than in HepaRG cells with both 100 and 20 nm microspheres.

Together, these data demonstrated that the uptake in HepaRG cells was more efficient for NPs of ca.100 nm than for smaller particles of ca. 30 nm, and strengthened the conclusion

than the PHB- and $PMLA_{800}$-*b*-PHB_{7300}-based NPs favored the HepaRG cell uptake while reducing it in macrophages.

In vitro cell biocompatibility towards PHB-b-PMLA and PTMC-b-PMLA based NPs

In previous reports, we demonstrated that acute and chronic incubations with NPs based on PMLA-*b*-PHB and PMLA-*b*-PTMC copolymers did not significantly affect the HepaRG cell viability using the MTT assay (Barouti et al., 2015; Barouti et al., 2016). In order to further characterize the biocompatibility of the nano-objects obtained from these two sets of copolymers, macrophages and HepaRG cells were incubated overnight with NPs to study the inflammasome activation levels through the production of pro-inflammatory cytokines (Figure 4).

Macrophages and HepaRG cells were cultured in the absence or presence of LPS for inflammasome priming, and monosodium urate (MSU) crystals were used as positive control of sustained inflammasome activation (Gicquel et al., 2015). In a first step, we measured the LDH release in culture media to determine whether the incubation with NPs in presence or absence of LPS affected the cell viability. The LDH activities were not significantly affected by the incubation with the NPs or the MSU treatment. The overall inflammation was evaluated by measuring the concentration of the pro-inflammatory cytokines IL-6 and IL-1α and the level of inflammasome activation was studied by determining the secretion of IL-1β in culture media of macrophages (Figure 4). For control cells in absence of priming, IL-6 was the only detectable cytokine. As expected, the priming with LPS slightly increased the secretion of the three cytokines but the incubation with PMLA-*b*-PHB and PMLA-*b*-PTMC-based NPs did not enhance the secretion of pro-inflammatory cytokines, thus demonstrating that these nano-objects did not activate the inflammasome in primary macrophages. In contrast, the treatment with MSU strongly triggered the inflammasome activation visualized by the increase in cytokine secretion, as previously reported (Gicquel et al 2015). The HepaRG cells produced much lower amounts of inflammation mediators and the IL6 was the only cytokine detectable in the culture medium. As observed for macrophages, priming with LPS slightly increased the secretion of IL-6 and the incubation with NPs did not significantly enhanced the secretion of IL-6 demonstrating that PMLA-*b*-PHB and PMLA-*b*-PTMC-based NPs did not activate the inflammasome in this hepatocyte-like model.

In vitro opsonisation of PHB-b-PMLA and PTMC-b-PMLA based NPs

The opsonisation of the PMLA-*b*-PHB and PMLA-*b*-PTMC-based NPs by human serum proteins was evaluated in a cell-free protein adsorption assay (Figure 5). In a first experiment, the protein adsorption by PHB- and PTMC-based NPs was evaluated over a 16 h time-course (Figure 5A). The proteins bound to the NPs obtained from both PHB and PTMC homopolymers were separated by electrophoresis and visualized by coomassie blue staining of polyacrylamide gels. A ladder of proteins with two major bands migrating at an apparent mobility of ca.70 and 25 kDa were bound onto NPs as early as 5 min after incubation with serum, and their abundance slowly increased with the incubation time. These two strong bands most likely corresponded to heavy and light chains of the immunoglobulins and the abundant plasma proteins such as the albumin.

A similar procedure was used to compare the opsonisation of NPs derived from $PMLA_{800}$-*b*-PHB_{7300}, $PMLA_{4500}$-*b*-PHB_{4400}, $PMLA_{2500}$-*b*-$PTMC_{2800}$, and $PMLA_{4300}$-*b*-$PTMC_{1400}$ copolymers and polystyrene microspheres (100 nm) after 15 and 60 min of incubation with human serum (Figure 5B). The PHB- and PTMC-homopolymer nano-objects exhibited a much stronger opsonisation compared to that of NPs prepared from PMLA-*b*-PHB and PMLA-*b*-PTMC copolymers and polystyrene microspheres. The NPs prepared with the PMLA-*b*-PHB copolymers generated the weakest opsonisation with bands which were barely detectable with NPs based on $PMLA_{4500}$-*b*-PHB_{4400}. Protein bands were observed with nano-objets of $PMLA_{800}$-*b*-PHB_{7300}, but they were less intense compared to the adsorption found with PMLA-*b*-PTMC-based NPs and polystyrene microspheres.

The evaluation of the protein adsorption by coomassie blue staining of polyacrylamide was completed by immunoblotting of plasma proteins (Figure 5C). Specific antibodies were used to detect the human albumin, transferrin and fibrinogen (known to bind to nano-objets non-specifically), the immunoglobulins and complement C3, which are part of the complement system activating phagocytic mononuclear cells upon binding to circulating antigens. As expected, an elevated abundance in albumin, transferrin, fibrinogen, immunoglobulins and complement C3 was found in samples of NPs formulated from PHB and PTMC homopolymers and PMLA-*b*-PTMC copolymers. The bands obtained were less intense when the serum was incubated with FluoSpheres® microspheres and weak for PMLA-*b*-PHB copolymers especially in samples of $PMLA_{4500}$-*b*-PHB_{4400}-based NPs.

Together, these data indicated that NPs derived from PHB and PTMC homopolymers were heavily opsonized, while the binding of plasmatic proteins was milder on nano-objects derived from PMLA-*b*-PTMC copolymers and very low for PMLA-*b*-PHB-based nanoobjects. This supported the conclusion that the hydrophilicity and the steric hindrance generated by the PMLA block is useful to reduce the opsonisation of the obtained NPs but also that the structure of hydrophobic block influences the binding of plasma proteins with the PMLA hydrophilic fraction.

Influence of the opsonisation of PMLA-b-PHB and PMLA-b-PTMC based NPs on cell uptake

It has been previously reported that the opsonization of polystyrene (Furumoto et al., 2002 ; Furumoto et al., 2004) and silica (Lesniak et al., 2012) NPs strongly affected the cell uptake. Given that the opsonisation by human plasmatic proteins considerably varied between PMLA-*b*-PTMC- and PMLA-*b*-PHB-derived NPs, we next investigated the influence of the opsonisation of NPs on the cell uptake by human macrophages and HepaRG hepatoma cells (Figure 6). To address this issue, "native" or opsonized DiDoil-loaded NPs or FluoSpheres® microspheres were used and the cell uptake was performed by culturing the macrophages and HepaRG cells in culture medium lacking fetal calf serum (FCS). The opsonized NPs were obtained by pre-incubating the "native NPs" with human serum prior to the dilution in the culture medium for the cell uptake.

As observed in Figure 1, the cell uptake by the macrophages was very efficient for all the nano-objects tested with at least 85% of positive cells except for the NPs formulated with the PTMC homopolymer (11% and 28% of positive macrophages with native and opsonized PTMC-based NPs, respectively). For the PHB-derived NPs, the opsonisation slightly reduced the number of positive cells (98% versus 85% for native and opsonized NPs, respectively). Interestingly, the mean of fluorescence in macrophages was not significantly affected by the pre-incubation of the NPs or FluoSpheres® microspheres with human serum when compared to the cell uptake of "native" NPs. In addition, the deprivation in FCS did not affect this cell uptake since the overall values of fluorescence in these experiments were very similar to those found in presence of 10% FCS (Figure 2).

As observed in macrophages, the uptake of NPs based on PHB-, PMLA-*b*-PTMC- and PMLA-*b*-PHB and FluoSpheres® beads was very efficient in HepaRG cells with more than

90% of positive cells. However, the opsonisation of nano-objects formulated from PHB homopolymer significantly reduced the mean of fluorescence with 98% and 70% for "native" and opsonized nanovectors, respectively. The number of positive cells with PTMC-based NPs remained low at ca. 8% for "native NPs and 2.5% for NPs pre-incubated with human serum. In contrast with the results obtained for macrophages, the means of fluorescence were significantly different for HepaRG cells incubated with native or opsonized NPs based on $PMLA_{800}$-*b*-PHB_{7300}, PMLA-*b*-PTMC and FluoSpheres® beads. The pre-incubation of NPs formulated with PMLA-*b*-PTMC and FluoSpheres® microspheres with human serum strongly decreased the uptake by HepaRG cells compared to that measured in cells incubated with native NPs. Unexpectedly, a 2.5-fold increase in the mean of fluorescence was found in cells incubated with opsonized $PMLA_{800}$-*b*-PHB_{7300}-based NPs compared to the fluorescence intensity measured for untreated NPs. Interestingly, the low HepaRG cell uptake observed for 20 nm FluoSpheres® beads compared to the very high uptake of 100 nm beads following opsonization by human plasma proteins (Figure 6) and in presence of FCS (Figure 3) was not significantly enhanced between the two different sizes of NPs in native FluoSpheres® beads (Figure 5).

All these data demonstrate that the uptake of NPs formulated with PMLA-*b*-PTMC- and PMLA-*b*-PHB copolymers is differently affected by the opsonisation in macrophages and HepaRG hepatoma cells. Indeed, while the opsonization of these nano-objets has not effect on the uptake by macrophages, the adsorption of plasmatic proteins on PMLA-*b*-PTMC- and PMLA-*b*-PHB-based NPs strongly affects the accumulation of NPs in HepaRG cells. Following opsonization, the NPs prepared from $PMLA_{800}$-*b*-PHB_{7300} diblock copolymer triggered the most efficient uptake in HepaRG hepatoma cells. These NPs are characterized by a short hydrophilic PMLA block (molar mass values of 800 $g.mol^{-1}$) and a much longer hydrophobic segment (molar mass values of 7300 $g.mol^{-1}$) featuring nano-objets with hydrodynamic diameter of 130 nm and a surface charge of -52 mV. Importantly, these experiments demonstrate that the $PMLA_{800}$-*b*-PHB_{7300}-based NPs promote a higher uptake in HepaRG hepatoma cells than in primary macrophages.

Mechanisms of cell uptake of $PMLA_{800}$-b-PHB_{7300}-based NPs in HepaRG cells

The cellular uptake of nanoparticles is usually an energy-dependent mechanism of endocytosis (Sahay et al., 2010). A set of experiments was performed in order to investigate whether the uptake of $PMLA_{800}$-*b*-PHB_{7300}-based NPs in HepaRG cells could also involve

endocytosis (Figure 7). The energy-dependent uptake and the endocytosis were studied by comparing the HepaRG cell uptake at 37 and 4 °C, and in absence or presence of two endocytosis inhibitors, the genistein and chlorpromazin. To avoid cell death in these culture conditions, cell uptake are measured for short periods of time, usually limited 3 to 4 h (Lühmann et al., 2008). Since all the experiments of cell uptake in this study were performed during 24 h, the time-course of the $PMLA_{800}$-*b*-PHB_{7300}-based NPs cell uptake was determine to demonstrate that a short incubation time of NPs triggered a significant cell uptake (Figure 7A). The cell uptake evidenced by the number of positive cells and the intensity of fluorescence measured by flow cytometry progressively increased between 1 and 8 hours to reach 40% of positive cells at 8 hours and strongly increased at 16 and 24 hours with 75 and 100% of positive cells, respectively. These data demonstrated that a short incubation time of HepaRG cells of 4 h with $PMLA_{800}$-*b*-PHB_{7300}-based NPs triggered enough cell uptake (25%) to investigate the effects of the cold and endocytosis inhibitors on NPs cellular entry.

HepaRG cells were incubated with $PMLA_{800}$-*b*-PHB_{7300}-based NPs and the cell uptake was compared at 37 and 4 °C for 4 h (Figure 7B). The intensity of fluorescence used to measure the cell uptake was strongly decreased in HepaRG cells maintained at 4 °C suggesting that the cellular entry of NPs required an energy-dependent process. To further demonstrate the involvement of endocytosis in the PMLA-*b*-PHB cellular entry, the uptake between control and genistein- and chlorpromazin-treated cells at 37 °C was compared. These two compounds are known to inhibit calveolae- and clathrin-mediated endocytosis, respectively (Sahay et al., 2010). The cell uptake of NPs was significantly decreased with these two compounds strongly suggesting that several pathways of endocytosis would be involved in the PMLA-*b*-PHB NPs cell uptake. The stable cell viability following the incubation at 4 °C and the treatment with endocytosis inhibitors was confirmed using an MTT assay (Figure 7C).

DISCUSSION

In the present work, we have further characterized NPs derived from PMLA-*b*-PHB (Barouti et al., 2015) and PMLA-*b*-PTMC (Barouti et al., 2016) diblock copolymers featuring different hydrophilic weight fraction, size and surface charge to study the influence of the chemical structure on the inflammasome activation, the opsonisation and the cell uptake of the NPs by primary macrophages and hepatocyte-like HepaRG cells.

Macrophages are critical components of the innate immune system that internalizes endogenous and exogenous antigens to eliminate pathogens and are the main source of interleukin-1 family cytokines, which mediate the inflammatory processes. Previous articles

have demonstrated that certain NPs induce the production of IL-1β and an inflammation process in human macrophages via the activation of the NLR pyrin domain containing 3 (NLRP3) inflammasome (Lunov et al., 2011; Baron et al., 2015). Unwanted phagocytosis of nano-objects by macrophages fully justifies the studies of the characteristics and structural determinants of NPs triggering cell uptake and downstream activation of signaling pathways resulting in cytokine production and inflammation. Our data demonstrated that NPs derived from both PMLA-*b*-PHB and PMLA-*b*-PTMC copolymers did not induce the production of neither IL-1α, IL-1β nor IL-6 in primary human macrophage. In HepaRG hepatoma cells, only the IL-6 was detectable in the culture medium and as observed for macrophages, its level was not increased upon cell incubation with NPs. Recent data have demonstrated that the activation of NLRP-3-dependent inflammasome requires two stimuli: an initial Toll-Like Receptor (TLR)-dependent stimulus inducing the transcription of the IL-1β gene, and the synthesis of the pro-IL-1β precursor prior to a second stimulus triggering the activation of the caspase 1-dependent cleavage of the pro-IL-1β and the cytokine secretion (Kanneganti et al., 2007; Gicquel et al., 2015). In our experimental conditions, as expected, a low dose of LPS used as a priming factor induced the production of IL1-α and IL-1β in macrophages, and IL-6 in both macrophages and HepaRG cells. However, incubation of primed cells with NPs prepared from PMLA-*b*-PHB and PMLA-*b*-PTMC copolymers did not further enhance the cytokine secretion indicating that these NPs do not significantly activate either the transcription of cytokine genes or the post-translational cleavage of pro-IL-1β.

Together, these data combined with the fact that NPs did not trigger LDH release, further strengthen the excellent biocompatibility of PMLA-*b*-PHB and PMLA-*b*-PTMC copolymer derived nano-objects as previously indicated using the mitochondrial activity MTT assay (Barouti et al., 2015; Barouti et al., 2016).

In this report, the opsonization of PMLA-*b*-PHB and PMLA-*b*-PTMC copolymers as well as PHB and PTMC homopolymers based NPs was investigated using an adapted cell-free protein adsorption assay (Nagayama et al., 2007 ; Du et al., 2015). Besides the fact that PHB and PTMC homopolymers self-assembled to form large objects incompatible with drug delivery purposes, the derived NPs were heavily opsonized. In contrast, the PMLA-*b*-PHB and PMLA-*b*-PTMC copolymers featuring a PMLA hydrophilic block and either a PHB or PTMC hydrophobic block, formed, as anticipated, much smaller NPs with different opsonization levels. The NPs prepared from $PMLA_{4500}$-*b*-PHB_{4400} and $PMLA_{2500}$-*b*-$PTMC_{2800}$ copolymers with hydrophilic fractions of f = ca. 50%, showed lower opsonization compared to that found

with NPs prepared from $PMLA_{800}$-*b*-PHB_{7300} and $PMLA_{4300}$-*b*-$PTMC_{1400}$, respectively. However, the most striking result was the very low opsonization observed for NPs derived from PMLA-*b*-PHB compared to the much higher protein adsorption found for PMLA-*b*-PTMC-based NPs, regardless of the hydrophilic fraction. These data demonstrate that the overall protein adsorption on nanoparticles prepared from these copolymers results not only from the hydrophilic/hydrophobic balance, but also from the chemical structures of the hydrophobic PHB (polyester) or PTMC (polycarbonate) block which strongly influence the interactions between the PMLA hydrophilic fraction and plasmatic proteins. Our results also emphasize that PMLA may represent a suitable alternative to the use of PEG as a hydrophilic block in the design of copolymers for NPs-mediated drug delivery. Although PEG is a widely used polymer (Veronese and Pasut, 2005), it showed some limitations related to its antigenicity, renal clearance and long-term toxicity (Dams et al., 2000; Kawai, 2002). The PMLA-based copolymers thus deserve more attention to determine their blood elimination, renal clearance and detailed nanotoxicological analysis in animal models to evaluate risk assessment, which remains poorly documented for nanotechnologies (Elsaesser and Howard, 2012).

A major aim of our study was to compare the cell uptake of PMLA-*b*-PHB and PMLA-*b*-PTMC copolymers based NPs by macrophages and HepaRG cells. In most experiments of cell uptake performed *in vitro*, the NPs are incubated with cells maintained in their standard culture medium containing 5 to 10 % of FCS (Zauner et al., 2001; Lunov et al., 2011 ; Baron et al., 2015). It is established that in these conditions, the NPs are rapidly opsonized by proteins of the FCS and that the opsonization affects the surface charges, the cell interactions and the cell uptake (Fleischer and Payne, 2015). In a first set of experiments, NPs derived from PMLA-*b*-PHB and PMLA-*b*-PTMC copolymers were incubated with macrophages and HepaRG cells in presence of 10% of FCS. The main conclusions were that the cell uptake efficiencies differed between the NPs and the two cell types and were not correlated to the DiD oil EE. The highest uptake in macrophages were observed for the two PMLA-*b*-PHB-based NPs. ~~In contrast~~ Similarly, the NPs prepared from the $PMLA_{800}$-*b*-$PHB_{7300,}$ exhibiting a hydrodynamic diameter of 130 nm, generated the highest accumulation in HepaRG hepatoma cells. The much lower uptake obtained with the $PMLA_{4500}$-*b*-PHB_{4400} derived NPs may arise from the small size of these NPs (30 nm) since FluoSpheres® beads of 20 nm were also weakly internalized compared to the efficient uptake observed with 100 nm beads. Conversely, the size of the PMLA-*b*-PHB-based NPs and FluoSpheres® beads had no significant effect on the uptake by macrophages. These results are in agreement with previous reports indicating that the *in vitro* uptake of polystyrene microspheres varies considerably with the size of the nano-objects and between

cell types (Zauner et al., 2001; Foged et al. 2005; Win and Feng, 2005). In addition, our preliminary experiments strongly suggest that the cell uptake, at least in HepaRG hepatoma cells, is an energy-dependent endocytosis that would involve both calveolae- and clathrin-mediated pathways, as previously observed for many polymeric NPs (Sahay et al., 2010).

The great differences observed in the opsonization levels of the NPs derived from PMLA-*b*-PHB and PMLA-*b*-PTMC copolymers prompted us to further investigate the effect of the NPs opsonisation by plasma proteins on the cell uptake. The opsonisation was performed using human plasma prior to the incubation with cells and the cell uptake was compared between native or opsonized NPs in culture medium lacking FCS. The recognition of antigens, including NPs, by the innate immune system in the body is mostly mediated by the binding of the opsonin proteins to the antigens (Frank and Fries, 1991; Owens and Peppas, 2006; Tenzer et al., 2013). It was thus unexpected to observe identical accumulations of native and opsonized PMLA-*b*-PHB and PMLA-*b*-PTMC-based NPs in macrophages. Furthermore, in macrophages, the levels in the uptake observed between the four NPs incubated in presence of 10% FCS were similar to those measured in cells incubated with native or opsonized NPs. These results indicate that in our experimental conditions, the cell uptake of NPs derived from PMLA-*b*-PHB and PMLA-*b*-PTMC copolymers by macrophages does not predominantly rely on the binding of opsonins but rather depends of the chemical structure and the intrinsic characteristics of the NPs.

In total contrast, the comparison of native and opsonized NPs uptake by HepaRG cells revealed the strong influence of the pre-coating of PMLA-*b*-PHB and PMLA-*b*-PTMC copolymers derived NPs by plasma proteins. While the uptake of NPs formulated from PMLA-*b*-PTMC copolymers was significantly decreased by opsonization, the internalization of NPs prepared from $PMLA_{800}$-*b*-PHB_{7300}, was strongly induced by serum pre-coating. Our data of protein adsorption combined with these results of cell uptake strongly suggest that the limited binding of a specific subset of plasmatic proteins by the PMLA-*b*-PHB-based NPs favors the cell uptake by HepaRG cells. Conversely, the high opsonization of PMLA-*b*-PTMC and polystyrene FluoSpheres® beads is most likely a key determinant in reducing the cell uptake in HepaRG cells since the accumulation of these NPs was increased in absence of FCS or pre-coating by human serum. Previous reports have also studied the influence of the opsonin binding onto polystyrene nanospheres on the hepatic disposition using a rat liver perfusion model (Furumoto et al., 2002; Furumoto et al., 2004; Ogawara et al., 2004; Nagayama et al., 2007). The authors in this different experimental model also demonstrated that opsonization of polystyrene NPs by serum proteins reduces the hepatic disposition of these NPs, while a pre-

coating of the nanospheres with purified human albumin prevented the binding of other plasma proteins and increased the blood circulation time. However, this model of liver perfusion including the intra-hepatic macrophages, the Kupffer cells, and the hepatocytes did not allow to discriminate the influence of the NPs opsonization on the cell uptake by macrophages versus hepatocyte-like cells. In that respect, our data demonstrated that the opsonization PMLA-*b*-PHB-based NPs has a positive effect on the uptake by the HepaRG cells while reducing that of macrophages. These results also strengthen the concept that actual development of new copolymers and optimized NPs design should minimize the clearance by MPS and improve tumor accumulation (Yang et al., 2016). In our study, the NPs prepared from $PMLA_{800}$-*b*-PHB_{7300} diblock copolymer exhibiting a hydrodynamic diameter of 130 nm and a surface charge of -52 mV triggered the most efficient uptake in HepaRG hepatoma cells.

The authors declare no financial or commercial conflict of interest.

ACKNOWLEDGEMENTS

The authors gratefully thank the Fondation pour la Recherche Médicale (FRM) (Ph.D. fellowship to G.B. and grant to K.J.), the Agence Régionale de Santé Pays de la Loire (1 year fellowship to E.V.) Institut National de la Santé et de la Recherche Médicale (Inserm) and the Centre National de la Recherche Scientifique (CNRS) for financial supports.

REFERENCES

Alving, C.R., Steck, E.A., Chapman, W.L., Waits, V.B., Hendricks, L.D., Swartz, G.M., Hanson, W.L., 1978. Therapy of leishmaniasis: superior efficacies of liposome-encapsulated drugs. Proc. Natl. Acad. Sci. 75, 2959-2963.

Arvizo, R.R., Miranda, O.R., Moyano, D.F., Walden, C.A., Giri, K., Bhattacharya, R., Robertson, J.D., Rotello, V.M., Reid, J.M., Mukherjee, P., 2011. Modulating pharmacokinetics, tumor uptake and biodistribution by engineered nanoparticles. PLoS One 6, e24374.

Asran, A.Sh., Razghandi, K., Aggarwal, N., Michler, G.H., Groth, T., 2010. Nanofibers from blends of polyvinyl alcohol and polyhydroxy butyrate as potential scaffold material for tissue engineering of skin. Biomacromolecules 11, 3413-3421.

Azzopardi, E.A., Ferguson, E.L., Thomas, D.W., 2013. The enhanced permeability retention effect: a new paradigm for drug targeting in infection. J. Antimicrob. Chemother. 68, 257-274.

Baron, L., Gombault, A., Fanny, M., Villeret, B., Savigny, F., Guillou, N., Panek, C., Le Bert, M., Lagente, V., Rassendren, F., Riteau, N., Couillin, I., 2015. The NLRP3 inflammasome is activated by nanoparticles through ATP, ADP and adenosine. Cell Death Dis. 6, e1629.

Barouti, G., Jarnouen, K., Cammas-Marion, S. Loyer, P., Guillaume, S.M., 2015. Polyhydroxyalkanoate-based amphiphilic diblock copolymers as original biocompatible nanovectors. Polym. Chem. 6, 5414-5429.

Barouti, G., Khalil, A., Orione, C., Jarnouen, K., Cammas-Marion, S., Loyer, P., Guillaume, S.M., 2016a. Poly(trimethylene carbonate)/Poly(malic acid) Amphiphilic Diblock Copolymers as Biocompatible Nanoparticles. Chem. Eur. J. 22, 2819-2830.

Barouti, G., Guillaume, S.M., 2016b. Polyhydroxyalkanoate (PHB)-based triblock copolymers: synthesis of hydrophobic PHB/poly(benzyl β-malolactonate) and amphiphilic PHB/poly(malic acid) analogues by ring-opening polymerization. Polym. Chem. 7, 4603-4608.

Barouti, G.,Liow, S.S., Dou, Q., Ye, H., Orione, C., Guillaume, S.M., Loh, X.J., 2016c. New linear and star-shaped thermogelling poly([R]-3-hydroxybutyrate) copolymers. Chem. Eur. J. 22, 10501-10512.

Blanco, E., Shen, H., Ferrari M., 2015. Principles of nanoparticles design for overcoming biological barriers to drug delivery. Nat. Biotech. 33, 941-951.

Cabral, H., Miyata, K., Kishimura, A., 2009. Nanodevices for studying nano-pathophysiology. Adv. Drug Delivery Rev. 2014, 74, 35-52.

Chen, W., Meng, F., Cheng, R., Deng, C., Feijen, J., Zhong, Z., 2014. Advanced drug and gene delivery systems based on functional biodegradable polycarbonates and copolymers. J. Control. Rel. 190, 398-414.

Corlu, A., Loyer, P., 2015. Culture Conditions Promoting Hepatocyte Proliferation and Cell Cycle Synchronization. Methods Mol. Biol. 1250, 27-51.

Dams, E.T., Laverman, P., Oyen, W.J., Storm, G., Scherphof, G.L., van Der Meer, J.W., Corstens, F.H., Boerman, O.C., 2000. Accelerated blood clearance and altered biodistribution of repeated injections of sterically stabilized liposomes. J. Pharmacol. Exp. Ther. 292, 1071-1079

Dawidczyk, C.M., Kim, C., Park, J.H., Russell, L.M., Lee, K.H., Pomper, M.G., Searson, P.C., 2014. State-of-the-art in design rules for drug delivery platforms: lessons learned from FDA-approved nanomedicines. J. Control. Rel. 187, 133-144.

Ding, Y., Li, W., Müller, T., Schubert, D.W., Boccaccini, A.R., Yao, Q., Roether, J.A., 2016. Electrospun Polyhydroxybutyrate/Poly(ε-caprolactone)/58S Sol-Gel Bioactive Glass Hybrid Scaffolds with Highly Improved Osteogenic Potential for Bone Tissue Engineering. ACS Appl. Mater. Interfaces. 8, 17098-17108.

Du, X.J., Wang, J.L., Liu, W.W., Yang, J.X., Sun, C.Y., Li, H.J., Shen, S., Luo, Y.L., Ye, X.D., Zhu, Y.H., Yang, X.Z., Wang, J., 2015. Regulating the surface poly(ethylene glycol) density of polymeric nanoparticles and evaluating its role in drug delivery in vivo. Biomaterials 69, 1-11.

Editorial., 2014. Time to deliver. Nat. Biotechnol. 32, 961.

Elsaesser, A., Howard, C.V., 2012. Toxicology of nanoparticles. Adv. Drug Deliv. Rev. 64, 129-137.

Fattal, E., Youssef, M., Couvreur, P., Andremont, A., 1989. Treatment of experimental salmonellosis in mice with ampicillin-bound nanoparticles. Antimicrob. Agents Chemother. 33, 1540-1543.

Fleischer, C.C., Payne, C.K., 2014. Nanoparticle-cell interactions: molecular structure of the protein corona and cellular outcomes. Acc Chem Res. 47, 2651-2659.

Foged C, Brodin B, Frokjaer S, Sundblad A., 2005. Particle size and surface charge affect particle uptake by human dendritic cells in an in vitro model. Int J Pharm. 298, 315-322.
Frank, M.M., Fries, L.F., 1991. The role of complement in inflammation and phagocytosis. Immunol. Today 12, 322-326.

Fukushima, K., 2016. Poly(trimethylene carbonate)-based polymers engineered for biodegradable functional biomaterials. Biomater Sci. 4, 9-24.

Furrer, P., Zinn, M., Panke, S., 2008. Polyhydroxyalkanoate and its potential for biomedical applications, Woodhead Publishing Ltd.: 2008; pp. 416-445.

Furumoto, K., Ogawara, K., Nagayama, S., Takakura, Y., Hashida, M., Higaki, K., Kimura, T., 2002. Important role of serum proteins associated on the surface of particles in their hepatic disposition. J. Control. Rel. 83, 89-96.

Furumoto, K., Nagayama, S., Ogawara, K., Takakura, Y., Hashida, M., Higaki, K., Kimura, T., 2004. Hepatic uptake of negatively charged particles in rats: possible involvement of serum proteins in recognition by scavenger receptor. J. Control. Rel. 97, 133-141.

Gicquel, T., Robert, S., Loyer, P., Victoni, T., Bodin, A., Ribault, C., Gleonnec, F., Couillin, I., Boichot, E., Lagente, V., 2015. IL-1β production is dependent on the activation of purinergic receptors and NLRP3 pathway in human macrophages. FASEB J. 29, 4162-73

Harris, J.M., Chess, R.B., 2003. Effect of pegylation on pharmaceuticals. Nat. Rev. 2, 214-221.

Hazer, B., 2010. Amphiphilic poly(3-hydroxy alkanoate)s: potential candidates for medical applications. Int. J. Polym. Sci. 2010, 1-8.

Huang, Z.W., Laurent, V., Chetouani, G., Ljubimova, J.Y., Holler, E., Benvegnu, T., Loyer, P., Cammas-Marion, S., 2012. New functional degradable and bio-compatible nanoparticles based on poly(malic acid) derivatives for site-specific anti-cancer drug delivery. Int. J. Pharm. 423, 84-92.

Ishida, T., Ichihara, M., Wang, X., Kiwada, H., 2006. Spleen plays an important role in the induction of accelerated blood clearance of PEGylated liposomes. J. Control. Rel., 115, 243-250.

Jacobs, F., Wisse, E., De Geest, B., 2010. The role of liver sinusoidal cells in hepatocyte-directed gene transfer. Am. J. Pathol. 176, 14-21.

Jiang, X., Xin, H., Gu, J., Xu, X., Xia, W., Chen, S., Xie, Y., Chen, L., Chen, Y., Sha, X., Fang, X., 2013. Solid tumor penetration by integrin-mediated pegylated poly(trimethylene carbonate) nanoparticles loaded with paclitaxel. Biomaterials 34, 1739-1746.

Kanneganti, T.D., Lamkanfi, M., Kim, Y.G., Chen, G., Park, J.H., Franchi, L., Vandenabeele, P., Núñez, G., 2007. Pannexin-1-mediated recognition of bacterial molecules activates the cryopyrin inflammasome independent of Toll-like receptor signaling. Immunity 26, 433-443

Kawai, F., 2002. Microbial degradation of polyethers. Appl. Microbial. Biotechnol. 58, 30-38.

Kierstead, P.H., Okochi, Venditto, V.J., Chuong, T.C., Kivimae, S., Fréchet, J.M.J.; Szola, F.C., 2015. The effect of polymer backbone chemistry on the induction of the accelerated blood clearance in polymer liposomes. J Control. Rel. 213, 1-9.

Kola, I., Landis, J., 2004. Can the pharmaceutical industry reduce attrition rates? Nat. Rev. 3, 711-715.

Lammers T, Ulbrich K., 2010. HPMA copolymers: 30 years of advances. Adv Drug Deliv Rev. 62, 119-121.

Lesniak, A., Fenaroli, F., Monopoli, M.P., Å, Dawson, K.A., Salvati, A., 2012. Effects of the presence or absence of a protein corona on silica nanoparticle uptake and impact on cell. ACS Nano 6, 5845-5857.

Li, Z., Loh, X. J., 2015. Water soluble polyhydroxyalkanoates: future materials for therapeutic applications. Chem. Soc. Rev., 44, 2865-2879.

Loyer, P., Cammas-Marion, S., 2014. Natural and synthetic poly(malic acid)-based derivates: a family of versatile biopolymers for the design of drug nanocarriers. J. Drug Target. 22, 556-575.

Lühman, T., Rimann, M., Bittermann, A.G., Hall, H., 2008. Cellular uptake and intracellular pathways of PLL-g-PEG-DNA. Bioconjugate Chem. 19, 1907-1916.

Lunov, O., Syrovets, T., Loos, C., Nienhaus, G.U., Mailänder, V., Landfester, K., Rouis, M., Simmet, T., 2011. Amino-functionalized polystyrene nanoparticles activate the NLRP3 inflammasome in human macrophages. ACS Nano. 5, 9648-9657.

Maeda, H., Nakamura, H., Fang, J., 2013. The EPR effect for macromolecular drug delivery to solid tumors: Improvement of tumor uptake, lowering of systemic toxicity, and distinct tumor imaging in vivo. Adv. Drug Deliv. Rev., 65, 71-79.

Maeda H., Tsukigawa K., Fang J., 2016. A retrospective 30 years after discovery of the enhanced permeability and retention effect to solid tumors: next-generation chemotherapeutics and photodynamic therapy-problems, solutions, and prospects. Microcirculation, 23, 173-182.
Mahon, E., Salvati, A., Baldelli Bombelli, F., Lynch, I., Dawson, K. A., 2012. Designing the nanoparticles-biomolecule interface for “targeting and therapeutic delivery”. J. Control. Rel. 161, 164-174.

Matsumura, Y. Maeda, H., 1986. A new concept for macromolecular therapeutics in cancer chemotherapy: mechanism of tumoritropic accumulation of proteins and the antitumor agent smancs. Cancer Res. 46, 6387-6392.

Misra R., Acharya S., Sahoo S. K., 2010. Cancer nanotechnology: application of nano-technology in cancer therapy. Drug Discov Today, 15, 842–850.

Moghini, S.M., Hunter, A.C., Murray, J.C., 2001. Long-circulating and target-specific nanoparticles: Theory to practice. Pharmacol. Rev. 53, 283-318.

Nagayama, S., Ogawara, K., Fukuoka, Y., Higaki, K., Kimura, T., 2007. Time-dependent changes in opsonin amount associated on nanoparticles alter their hepatic uptake characteristics. Int J Pharm. 342, 215-221.

Nel, A.E., Mädler, L., Velegol, D., Xia, T., Hoek, E.M., Somasundaran, P., Klaessig, F., Castranova, V., Thompson, M., 2009. Understanding biophysicochemical interactions at the nano-bio interface. Nat. Mater. 8, 543-557.

Nigmatullin, R., Thomas, P., Lukasiewicz, B., Puthussery, H., Roy, I., 2015. Polyhydroxyalkanoates, a family of natural polymers, and their applications in drug delivery. J. Chem. Technol. Biotechnol. 90, 1209-1221.

O'Brien, M.E., Wigler N, Inbar M, Rosso R, Grischke E, Santoro A, Catane R, Kieback DG, Tomczak P, Ackland SP, Orlandi F, Mellars L, Alland L, Tendler C., 2004. Reduced cardiotoxicity and comparable efficacy in a phase III trial of pegylated liposomal doxorubicin HCl (CAELYX/Doxil) versus conventional doxorubicin for first-line treatment of metastatic breast cancer. Ann. Oncol. 15, 440-449.

Ogawara, K., Furumoto, K., Nagayama, S., Minato, K., Higaki, K., Kai, T., Kimura, T., 2004. Pre-coating with serum albumin reduces receptor-mediated hepatic disposition of polystyrene nanosphere: implications for rational design of nanoparticles. J. Control. Rel. 100, 451-455.

Owens, D.E., Peppas, N.A., 2006. Opsonization, biodistribution, and pharmacokinetics of polymeric nanoparticles. Int. J. Pharm. 307, 93-102.

Raemdonck, K., De Smedt, S.C., 2015. Lessons in simplicity that should shape the future of drug delivery. Nat. Biotechnol. 33, 1026-1027.

Paşcu, E.I., Cahill, P.A., Stokes, J., McGuinness, G.B., 2016. Towards functional 3D-stacked electrospun composite scaffolds of PHBV, silk fibroin and nanohydroxyapatite: Mechanical properties and surface osteogenic differentiation. J. Biomater. Appl. 30, 1334-1349.

Pramual, S., Assavanig, A., Bergkvist, M., Batt, C.A., Sunintaboon, P., Lirdprapamongkol, K., Svasti, J., Niamsiri, N., 2016. Development and characterization of bio-derived polyhydroxyalkanoate nanoparticles as a delivery system for hydrophobic photodynamic therapy agents. J. Mater. Sci. Mater. Med. 27(2):40.

Reddy, L. H., Couvreur, P., 2011. Nanotechnology for therapy and imaging of liver diseases. J. Hepatol. 55, 1461-1466.

Richter, A.W., Akerblom, E., 1984. Polyethylene glycol reactive antibodies in man: titer distribution in allergic patients treated with monomethoxy polyethylene glycol modified allergens or placebo, and in healthy blood donors. Int. Arch. Allergy Appl. Immunol. 74, 36-39.

Rozila, I., Azari, P., Munirah, S., Wan Safwani, W.K., Gan, S.N., Nur Azurah, A.G., Jahendran, J., Pingguan-Murphy, B., Chua, K.H., 2016. Differential osteogenic potential of human adipose-derived stem cells co-cultured with human osteoblasts on polymeric microfiber scaffolds. J. Biomed. Mater. Res. 104, 377-387.

Sahay, G., Alakhova, D.Y., Kabanov, A. V., 2010. Endocytosis of nanomedicines. J. Control. Rel. 145, 182-195.

Schüller-Ravoo, S., Teixeira, S.M., Feijen, J., Grijpma, D.W., Poot, A.A., 2013. Flexible and elastic scaffolds for cartilage tissue engineering prepared by stereolithography using poly(trimethylene carbonate)-based resins. Macromol. Biosci. 13, 1711-1719.

Shishatskaya, E.I., Volova, T.G., 2004. A comparative investigation of biodegradable polyhydroxyalkanoate films as matrices for in vitro cell cultures. J Mater Sci Mater Med. 15, 915-23.

Shrivastav, A., Kim, H.-Y., Kim, Y.-R., 2013. Advances in the applications of polyhydroxyalkanoate nanoparticles for novel drug delivery system. BioMed Res. Int. 1-12.

Song, Y., Wennink, J.W., Kamphuis, M.M., Sterk, L.M., Vermes, I., Poot, A.A., Feijen, J., Grijpma, D.W., 2011. Dynamic culturing of smooth muscle cells in tubular poly(trimethylene carbonate) scaffolds for vascular tissue engineering. Tissue Eng Part A 17, 381-387.

Stinchcombe, T.E., 2007. Nanoparticle albumin-bound paclitaxel: a novel Cremphor-EL-free formulation of paclitaxel. Nanomedicine 4, 415-423.

Tenzer, S., Docter, D., Kuharev, J., Musyanovych, A., Fetz, V., Hecht, R., Schlenk, F., Fischer, D., Kiouptsi, K., Reinhardt, C., Landfester, K., Schild, H., Maskos, M., Knauer, S.K., Stauber, R.H., 2013. Rapid formation of plasma protein corona critically affects nanoparticle pathophysiology. Nat. NanoTechnol. 8, 772-781.

Thioune, O., Fessi, H., Devissaguet, J. P., Puisieux, F., 1997. Preparation of pseudolatex by nanoprecipitation: influence of the solvent nature on intrinsic viscosity and interaction constant. Int. J. Pharm. 146, 233-238.

Torchilin V. P., 2006. Multifunctional nanocarriers. Adv Drug Deliv Rev, 58, 1532-1555.

Veronese, F.M., 2001. Peptide and protein PEGylation: a review of problems and solutions. Biomaterials 22, 405-417.

Veronese, F.M., Pasut, G., 2005. PEGylation, successful approach to drug delivery. Drug Discov Today. 10, 1451-1458.

Win, K.Y., Feng, S.S., 2005. Effects of particle size and surface coating on cellular uptake of polymeric nanoparticles for oral delivery of anticancer drugs. Biomaterials 26, 2713-2722.

Wu, Q., Wang, Y., Chen, G.-Q., 2009. Medical application of microbial biopolyesters polyhydroxyalkanoates. Artif. Cells Blood Substitutes Biotechnol. 37, 1-12.

Xiong, Y.C., Yao, Y.C., Zhan, X.Y., Chen, G.Q., 2010. Application of polyhydroxyalkanoates nanoparticles as intracellular sustained drug-release vectors. J. Biomater. Sci. Polym. Ed. 21, 127-140.

Yang B, Han X, Ji B, Lu R., 2016. Competition between tumor and mononuclear phagocyte system cause the low tumor distribution of nanoparticles and strategies to improve tumor accumulation. Curr. Drug Deliv. 13, publication ahead of printing. DOI: 10.2174.

Zant, E., Grijpma, D.W., 2016. Synthetic Biodegradable Hydrogels with Excellent Mechanical Properties and Good Cell Adhesion Characteristics Obtained by the Combinatorial Synthesis of Photo-Cross-Linked Networks. Biomacromolecules 17, 1582-1592.

Zauner, W, Farrow, NA, Haines, AM., 2001. In vitro uptake of polystyrene microspheres: effect of particle size, cell line and cell density. J Control. Rel. 71, 39-51.

Zhang, X., Ng, H.L., Lu, A., Lin, C., Zhou, L., Lin, G., Zhang, Y., Yang, Z., Zhang, H., 2016. Drug delivery system targeting advanced hepatocellular carcinoma: Current and future. Nanomedicine 12, 853-869.

Zelikin, A.N., Such, G.K., Postma, A., Caruso, F., 2007. Poly(vinylpyrrolidone) for bioconjugation and surface ligand immobilization. Biomacromolecules 8, 2950-2953.

LEGENDS OF FIGURES

Figure 1: *Structure of PMLA-b-PHB and PMLA-b-PTMC copolymers*

Figure 2: *Visualisation of the uptake of NPs derived from PHB and PTMC homopolymers and PMLA-b-PHB copolymers in primary macrophages and HepaRG hepatoma cells by flow cytometry and fluorescence microcopy*. The flow cytometry analysis was performed using 10^5 gated viable cells (gate R1 on the side scatter versus forward scatter dot plots, left column). The intrinsic FL4-H fluorescence of macrophages and HepaRG cells was set up using cells that were not incubated with NPs (w/o NPs, dotted line histograms) to define the M1 gate corresponding to negative cells. The fluorescence of macrophages and HepaRG cells incubated with DiD oil loaded NPs prepared from PHB and PTMC homopolymers, $PMLA_{800}$-*b*-PHB_{7300}, $PMLA_{4500}$-*b*-PHB_{4400}, $PMLA_{2500}$-*b*-$PTMC_{2800}$ and $PMLA_{4300}$-*b*-$PTMC_{1400}$ copolymers, and FluoSpheres® beads, was measured using the FL4-H channel to identify the positive cells in the M2 gate. Only overlay histograms of cells w/o NPs and cells incubated with $PMLA_{800}$-*b*-PHB_{7300}, $PMLA_{4500}$-*b*-PHB_{4400} and FluoSpheres® beads of 20 nm (MS20) and 100 nm (MS100) are presented. Fluorescence DiD oil loaded NPs (red) and FluoSpheres® microspheres (green) in macrophages and HepaRG cells were also detected by fluorescence microscopy: live cells in phase contrast microscopy are presented in the third column and the corresponding fluorescence photographs resulting from the accumulation of NPs into the cells are presented in the fourth column (magnification bar : 100nm).

Figure 3: *Analysis of the uptake of NPs derived on PHB and PTMC homopolymers, and PMLA-b-PHB and PMLA-b-PTMC copolymers, based in primary macrophages and HepaRG hepatoma cells measured by flow cytometry.* Charts represent the percentage of positive macrophages and HepaRG cells present in the M2 gate (see Figure 1) and the mean of fluorescence in arbitrary units (A.U.) in the positive cells following an overnight incubation with DiD oil loaded NPS. All the cells that were not incubated with NPs (w/o NPs) were considered negative and the mean of fluorescence was the mean of the all cells population. Macrophages prepared from two healthy donners were used to measure the uptake in 6 to 8 independent culture wells. Three independent cultures of HepaRG were performed to measure the uptake in 6 to 9 independent culture wells. * $p < 0.05$, ** $p < 0.01$.

Figure 4: *LDH release and concentrations in pro-inflammatory cytokines in culture media of macrophages and HepaRG cells*. The cytotoxicity of NPs derived from PHB and PTMC homopolymers, and PMLA-*b*-PHB and PMLA-*b*-PTMC copolymers, was measured by the LDH release in culture media of macrophages and HepaRG cells in absence (white bars) or presence (dark bars) of the inflammasome priming factor LPS. The inflammasome activation levels were studied by measuring the concentration in IL-6, IL-1α and IL1-β by Elisa assay. Number of experiments, macrophages n = 6 to 8 independent culture wells, HepaRG cells = 6 to 9 independent culture wells. * $p < 0.05$, ** $p < 0.01$.

Figure 5: *Opsonisation of NPs derived from PHB and PTMC homopolymers, and PMLA-b-PHB and PMLA-b-PTMC copolymers by plasmatic proteins from human serum*. A) PHB- and PTMC-based NPs were used to define the time course of the opsonisation assay. Incubation of NPs were performed at 5, 15, 30 min and 1, 2, 8 and 16 h. Adsorbed proteins were loaded on SDS-PAGE and the gels were stained with Coomassie blue. Molecular weight markers (M) indicate the apparent mobility range after electrophoresis. Serum input (S, 1:1000), control NPs that were not incubated with serum (CT). B) Qualitative analysis for serum proteins adsorbed on 100 nm FluoSpheres® microspheres (MS100) and NPs derived from PHB and PTMC homopolymers and PMLA-*b*-PHB- and PMLA-*b*-PTMC copolymers following 15 and 60 min of incubation with human serum. C) Immunodetection by western blotting of albumin, transferrin, fibrinogen, immunoglobulin light chains and complement C3 adsorbed on FluoSpheres® microspheres (MS100) and NPs derived from PHB, PTMC, PMLA-*b*-PHB- and PMLA-*b*-PTMC polymers.

Figure 6: *Effects of the opsonisation of NPs derived from PHB and PTMC homopolymers and PMLA-b-PHB and PMLA-b-PTMC copolymers by plasmatic proteins from human serum on the cell uptake by macrophages and HepaRG cells.* Charts represent the percentage of positive macrophages and HepaRG cells present in the M2 gate (see Figure 1), and the mean of fluorescence in arbitrary units (A.U.) in the positive cells following an overnight incubation with DiD oil-loaded NPs. The cells were cultured in absence of FCS and were either incubated with native NPs (white bars) or NPs pre-incubated with human serum (dark bars) for 30 min prior to the dilution in the culture medium. Number of experiments, macrophages n = 6 to 8 independent culture wells, HepaRG cells = 6 to 9 independent culture wells. * $p < 0.05$, ** $p < 0.01$.

Figure 7: *Inhibition of PMLA$_{800}$-b-PHB$_{7300}$–based NPs uptake in HepaRG cells.* A) Time-course of the PMLA$_{800}$-b-PHB$_{7300}$–based NPs uptake in HepaRG cells. Graphs represent the percentage of positive HepaRG cells and the mean of fluorescence in arbitrary units (A.U.) in the positive cells following incubation with DiD oil-loaded NPs at 1, 2, 4, 8, 16 and 24 h. B) The effects of genistein (200 µM), chlorpromazin (20 µM) and culture at 4 °C (cold) on the HepaRG cell uptake of the PMLA$_{800}$-b-PHB$_{7300}$–based NPs. Charts represent the mean of fluorescence in arbitrary units (A.U.) in the positive HepaRG cells following a 4 h incubation with DiD oil-loaded NPs. C) The effects of genistein (200 µM), chlorpromazin (20 µM) and culture at 4 °C (cold) on the HepaRG cell viability The mitochondrial assay MTT activities were presented in % of the control cells without treatment and cultured at 37 °C. Number of experiments, HepaRG cells = 4 independent culture wells. ** $p < 0.01$.

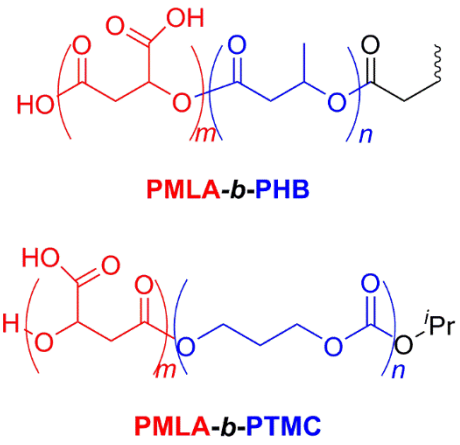

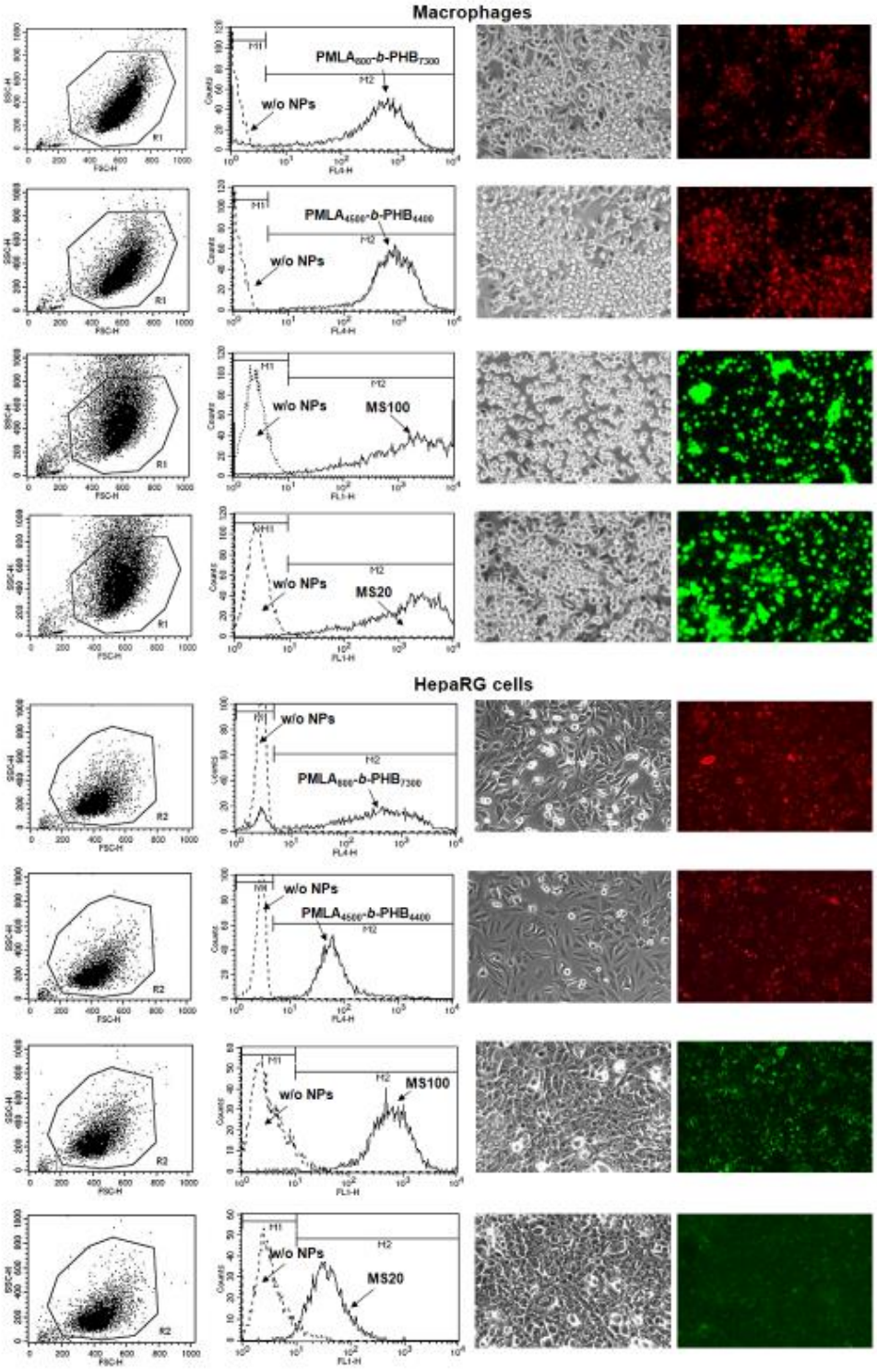

Figure 2

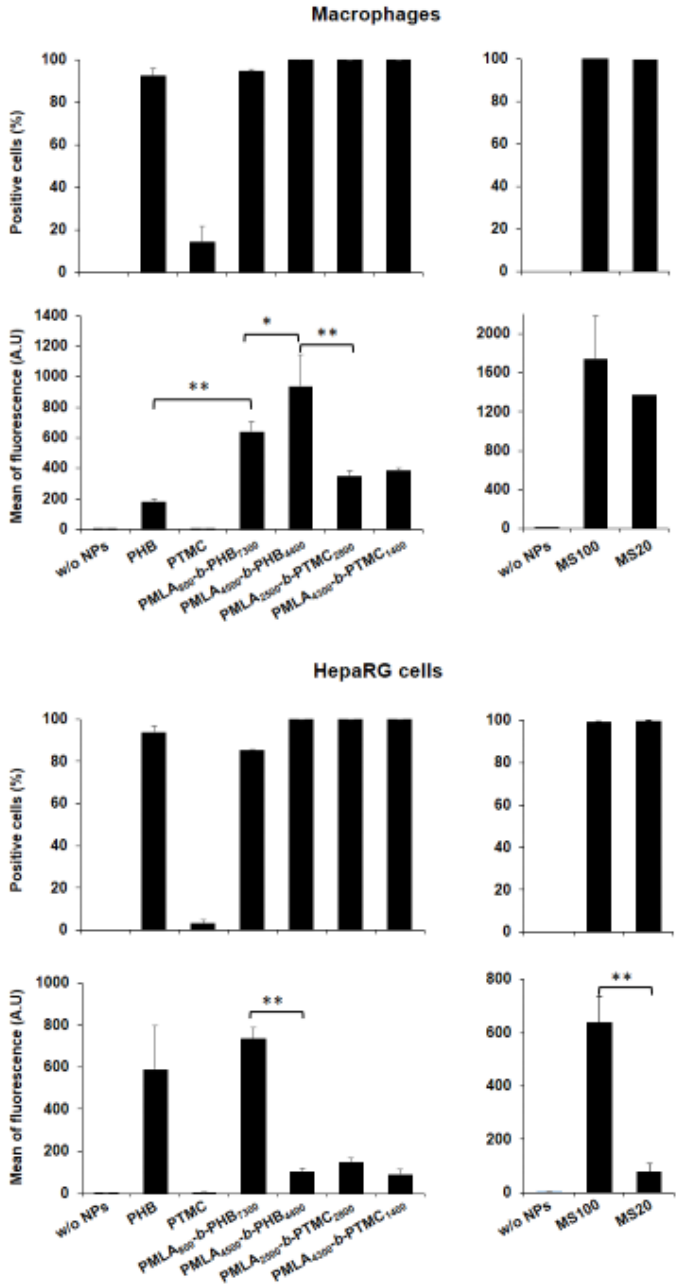

Figure 3

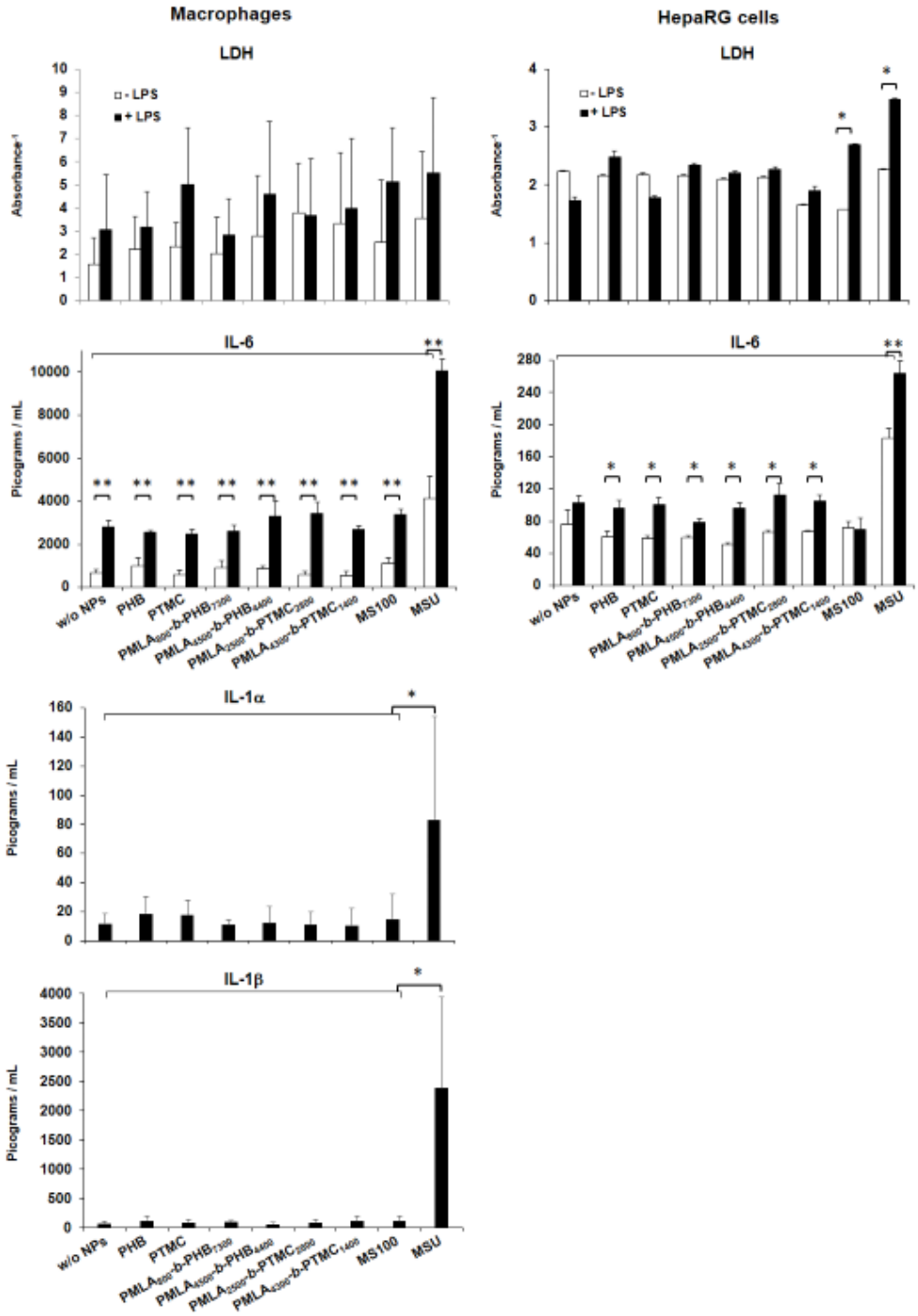

Figure 4

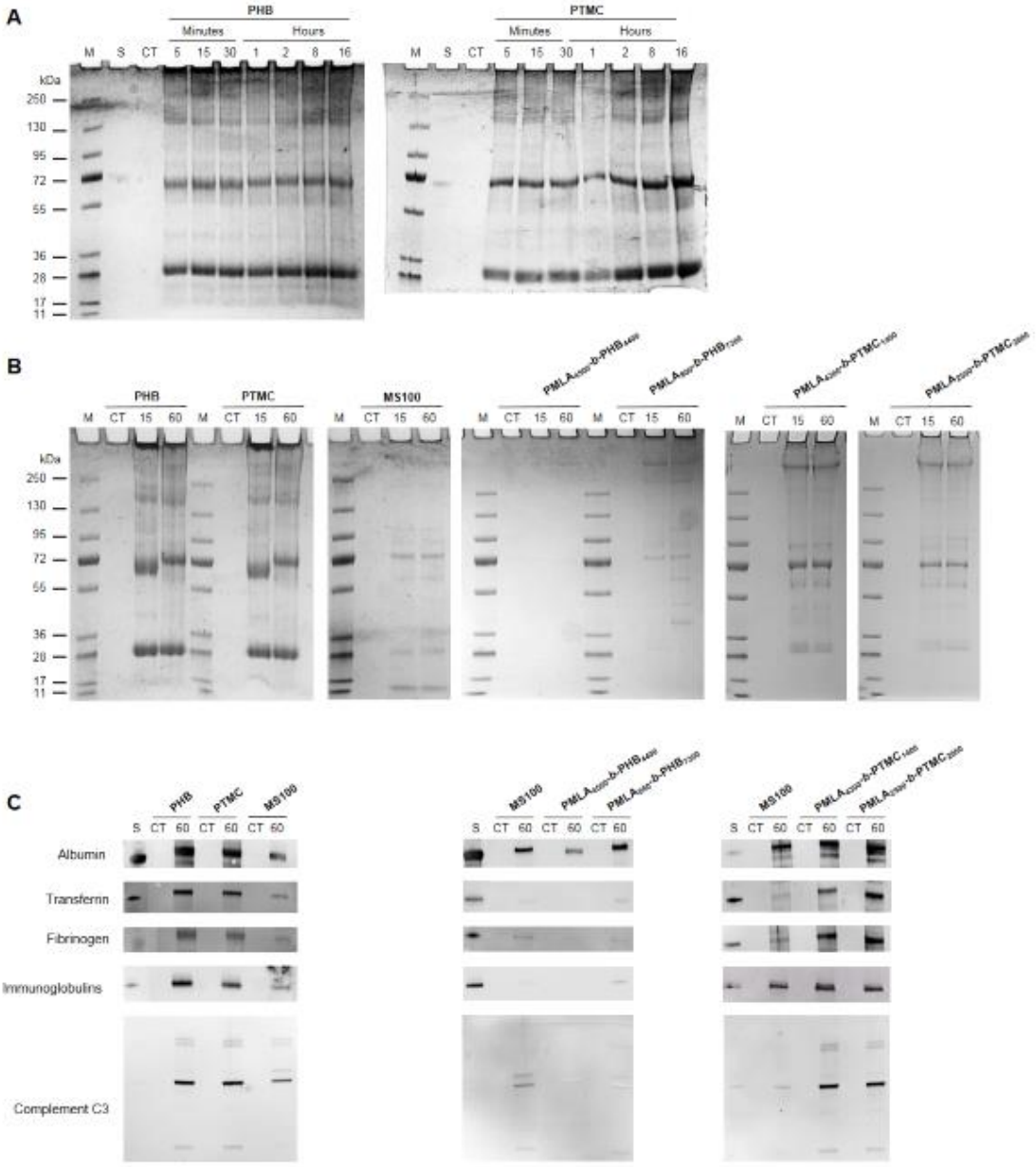

Figure 5

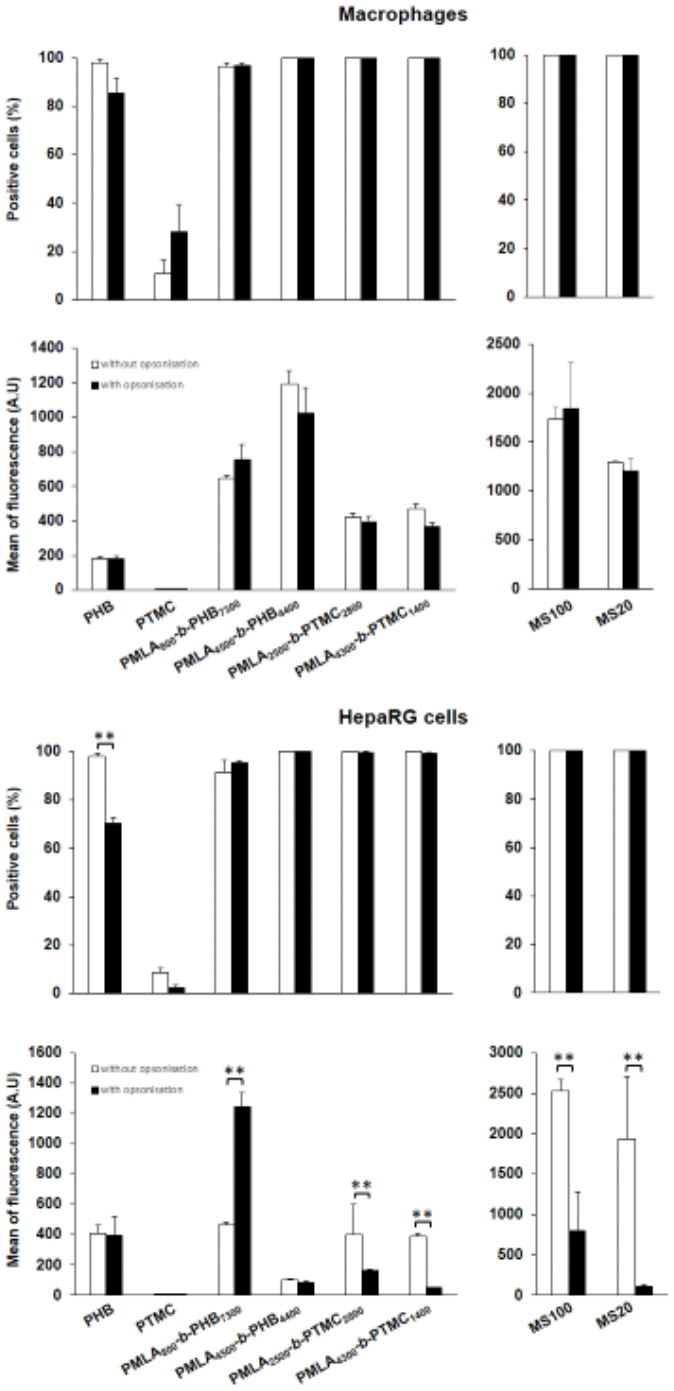

Figure 6

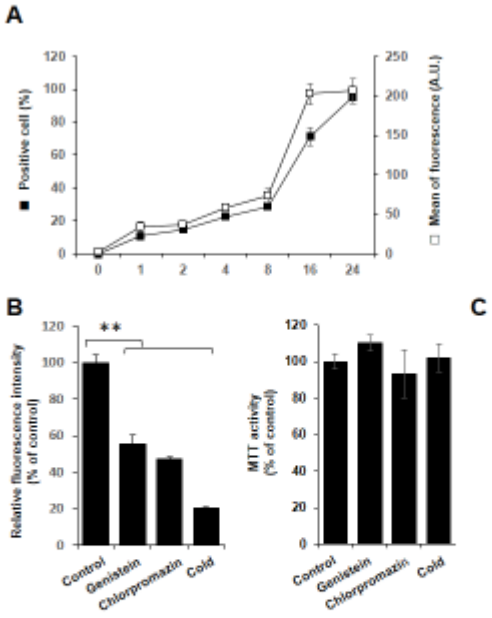

Figure 7

Table 1: *Characteristics of the NPs based on PHB and PTMC homopolymers, and PMLA-b-PHB and PTMC-b-PMLA copolymers*. [a] Experimental molar mass values of the PMLA-*b*-PHB determined by ^{1}H NMR analysis of the isolated polymers. [b] Hydrophilic weight fraction of copolymers (*f*). [c] Concentration of the PMLA-*b*-PHB copolymer in PBS. [d] Hydrodynamic diameter measured by DLS. [e] Polydispersity index of the NP size measured by DLS. [f] Zeta potential (ζ) measured from the electrophoretic mobility (μ) using the Smoluchowski approximation. [g] Encapsulation efficiency (EE) of the DiD oil in NPs measured by UV at 660 nm.

Polymer	$M_{n,NMR}$ [a] (g.mol^{-1})	f [b] (%)	[Polymer]$_0$ [c] (mg.mL^{-1})	D_h [d] (nm)	PDI [e]	ζ [f] (mV)	EE [g] (%)
PHB$_{2000}$	2000	-	2	544	0.2	ND	19
PTMC$_{3000}$	3000	-	2	956	0.4	ND	14.8
PMLA$_{800}$-*b*-PHB$_{7300}$	8100	10	2	130	0.2	−52	27.2
PMLA$_{4500}$-*b*-PHB$_{4400}$	8900	51	2	30	0.2	−50	45.2
PMLA$_{2500}$-*b*-PTMC$_{2800}$	5300	47	2	70	0.2	−26	32.6
PMLA$_{4300}$-*b*-PTMC$_{1400}$	5700	75	2	99	0.1	−18	39